Report

Current Biology

Early-life viability selection targets deleterious mutations in exons

Graphical abstract

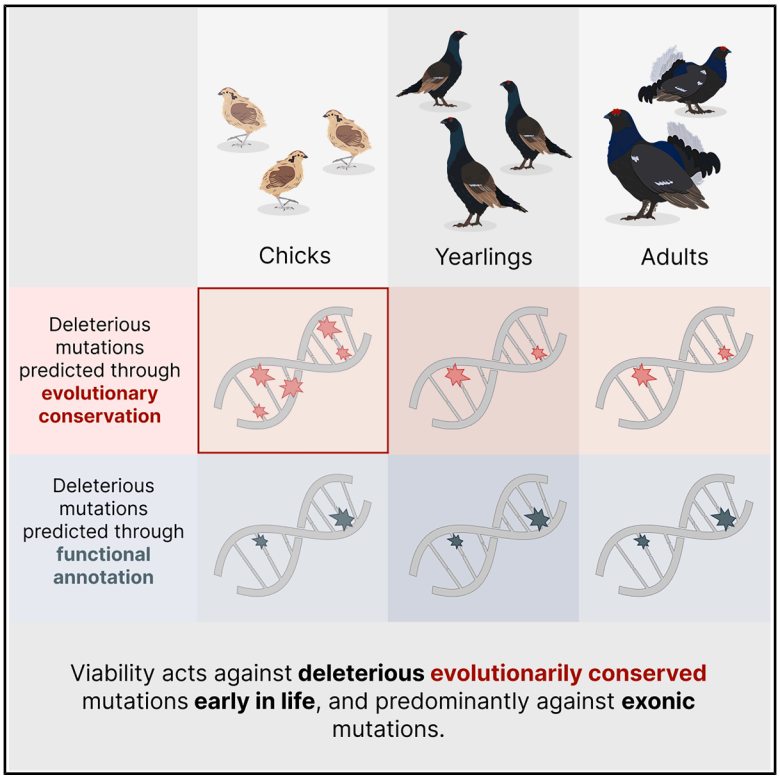

Highlights

- Viability selection against deleterious mutations occurs mostly early in life
- Viability selection targets evolutionarily conserved mutations in exonic regions

Authors

Rebecca S. Chen, Carl D. Soulsbury, Kees van Oers, Joseph I. Hoffman

Correspondence

rebecca.chen@uni-bielefeld.de

In brief

Chen et al. predict deleterious mutations in male black grouse chicks, yearlings, and adults. Their findings show that viability selection against these mutations acts mainly between the chick and yearling stages and specifically targets evolutionarily conserved mutations located in exonic regions.

Chen et al., 2025, Current Biology *35*, 5908–5914
December 1, 2025
https://doi.org/10.1016/j.cub.2025.10.043

CellPress

CellPress
OPEN ACCESS

Current Biology

Report

Early-life viability selection targets deleterious mutations in exons

Rebecca S. Chen,[1,8,*] Carl D. Soulsbury,[2] Kees van Oers,[3,4] and Joseph I. Hoffman[1,5,6,7]
[1]Department of Evolutionary Population Genetics, Faculty of Biology, Bielefeld University, 33501 Bielefeld, Germany
[2]School of Life and Environmental Sciences, Joseph Banks Laboratories, University of Lincoln, Lincoln LN67DL, UK
[3]Department of Animal Ecology, Netherlands Institute of Ecology (NIOO-KNAW), 6708PB Wageningen, the Netherlands
[4]Behavioural Ecology Group, Wageningen University & Research (WUR), 6708PB Wageningen, the Netherlands
[5]Center for Biotechnology (CeBiTec), Faculty of Biology, Bielefeld University, 33615 Bielefeld, Germany
[6]Joint Institute for Individualisation in a Changing Environment (JICE), Bielefeld University and University of Münster, 33615 Bielefeld, Germany
[7]British Antarctic Survey, High Cross, Madingley Road, Cambridge CB3OET, UK
[8]Lead contact
*Correspondence: rebecca.chen@uni-bielefeld.de
https://doi.org/10.1016/j.cub.2025.10.043

SUMMARY

Understanding how deleterious mutations affect fitness is central to evolutionary and conservation biology.[1,2] However, most empirical studies rely on inbreeding as a proxy for the mutation load,[3] overlooking the substantial contribution of deleterious mutations expressed in the heterozygous state.[4–6] Moreover, although mutations in coding and non-coding regions of the genome are hypothesized to have qualitatively different fitness effects and thus experience distinct selective pressures,[7] such functional heterogeneity is often overlooked. Selection may also vary across life stages, adding a temporal dimension that is seldom captured.[8,9] Using whole-genome resequencing data from the black grouse (*Lyrurus tetrix*), we predicted deleterious mutations using evolutionary conservation[10] and functional predictions.[11] We then used the resulting genomic mutation load estimates to quantify viability selection at functionally distinct genomic regions across three life-history stages: chicks, yearlings, and adults. We found that viability selection is strongest early in life and mainly targets deleterious mutations at evolutionarily conserved sites. Specifically, early-life selection predominantly acts against deleterious mutations located in exons, contrasting with our previous finding that sexual selection in this species targets deleterious mutations in regulatory regions.[6] These results show that the fitness effects of deleterious mutations are neither temporally constant nor uniformly distributed across the genome. Instead, they reflect dynamic selection regimes that shift across both life-history stages and genomic contexts. Our findings refine our understanding of evolutionary dynamics and life-history evolution, while also informing the use of genomic fitness indicators in biological conservation.

RESULTS

We sequenced the genomes of 236 male black grouse (*Lyrurus tetrix*) sampled from five leks in central Finland and assigned them to three age classes: chicks (n = 46), yearlings (n = 39), and adults (n = 151). We focused on males because they experience higher juvenile mortality than females[12] and are the philopatric sex,[13–15] allowing for more reliable long-term tracking. Chicks were sampled in the nest shortly after hatching. Yearlings were defined as birds aged 1 calendar year (Figure 1A); although not fully grown and typically not exhibiting territorial behavior, yearlings can occasionally achieve copulations.[16] Adults were defined as individuals aged 2 calendar years or older (Figure 1A); they are fully grown and engage in territorial behavior during the lekking season, depending on their body condition. We designated two distinct life-history stages: "early-life" (chick to yearling), a period of high mortality (survival rate: 11%–17%[12]), and "late life" (yearling to adult), when survival rates increase substantially (46%–70%[17–19]). Sequencing to an average coverage of 29× generated 58.5 billion 150 bp paired-end Illumina reads, which were used to call 7,245,059 high-quality SNPs. One chick genome was excluded from further analysis due to its high relatedness to a yearling genome ($\hat{p}$ = 0.96), indicating likely inadvertent resampling.

Viability selection acts during early life

To test for viability selection, we took a multilayered approach, starting by quantifying each individual's genomic inbreeding coefficient F_{ROH}, defined as the proportion of the autosomal genome contained in runs of homozygosity (ROHs). Across all individuals, we identified a total of 2,517,951 ROHs (minimum length = 100 kb; ≥100 SNPs), yielding F_{ROH} values ranging from 0.13 to 0.36 (mean = 0.15; Figure S1A). We then used Bayesian linear mixed-effect models (LMMs) of F_{ROH} to quantify inbreeding depression at both life-history stages. For early-life

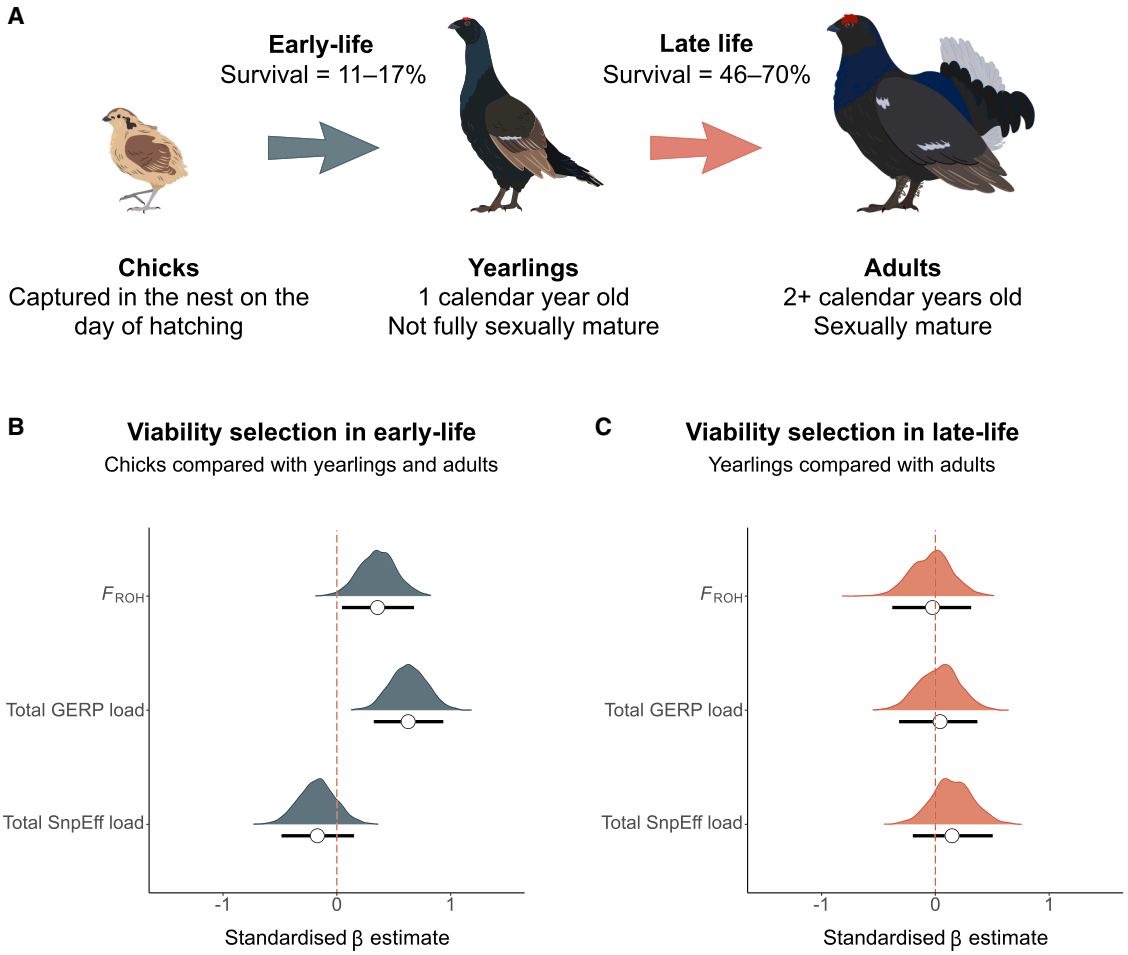

Figure 1. Differences in inbreeding and genomic mutation loads among chicks, yearlings, and adults

(A) Visual representation of the two life-history stages (early life versus late life) and the three age classes (chicks, yearlings, and adults).

(B) Posterior distributions of the standardized β estimates of age (chicks compared with yearlings and adults combined) on genomic inbreeding (F_{ROH}), the total GERP load, and the total SnpEff load (top to bottom).

(C) Posterior distributions of the standardized β estimates of age (yearlings compared with adults) on F_{ROH}, the total GERP load, and the total SnpEff load (top to bottom). The white circles represent the median posterior estimates and the horizontal black lines the 95% credible intervals (CIs).

See also Figure S1 and Table S2.

inbreeding depression, age class was modeled as a two-level fixed effect predictor variable, with chicks being compared with yearlings and adults combined. For late-life inbreeding depression, the same model structure was used to compare yearlings with adults. Lekking site was included as a random effect in both models to account for site-specific demographic variation.

In the early-life model, the posterior estimates of age were mostly positive, with a median β of 0.36 (95% credible interval [CI] = 0.05, 0.68; Table S2), indicating that chicks are significantly more inbred than older individuals (Figure 1B). In the late-life model, the 95% CI of the posterior estimates of age overlapped zero (median $\beta = -0.02$, 95% CI = −0.38, 0.31; Table S2), indicating no detectable difference in inbreeding between yearlings and adults (Figure 1C). Together, these results suggest that inbreeding depression is generally weak but may be more pronounced during early life, consistent with stronger viability selection acting against chicks.

To quantify the fitness effects of predicted deleterious mutations, we estimated each individual's genomic mutation load using two complementary approaches. The first was based on evolutionary conservation using GERP++, which assumes that mutations in evolutionarily conserved genomic regions are deleterious.[10] The second approach was based on functional annotation with SnpEff,[11] which classifies mutations as deleterious when they are predicted to cause a loss of function (LOF) or introduce premature stop codons, indicating a high functional impact on the encoded protein.

GERP++ identified a total of 415,115 mutations with a GERP score ≥ 4 (Figure S1B), while SnpEff identified a total of 5,296 high-impact mutations (Figure S1C), including LOF mutations, gained stop codons, and nonsense-mediated decay mutations (Figure S1D). For both approaches, we quantified each individual's total genomic mutation load as the number of derived deleterious mutations, summing across both homozygous and heterozygous sites (Figure S1A). Mutation load estimates from the

two approaches were not significantly correlated (Pearson's correlation coefficient = 0.07, $p = 0.29$). Likewise, mutation loads did not differ significantly among birds sampled from different lekking sites (Figure S2; Table S1) or born in different years (Figure S2; Table S1). As expected, more inbred individuals carried a greater number of deleterious mutations within ROHs, both for GERP (Pearson's correlation coefficient = 0.88, $p < 0.001$) and SnpEff mutations (Pearson's correlation coefficient = 0.84, $p < 0.001$).

To quantify viability selection against deleterious GERP mutations, we modified the Bayesian LMMs described above by replacing F_{ROH} with the total GERP load as the response variable. In the early-life model, the posterior estimates of age were consistently negative, with a median β of 0.63 (95% CI = 0.32, 0.94; Table S2), indicating that chicks carry significantly higher total GERP loads than older individuals (Figure 1B). By contrast, in the late-life model, the posterior estimates of age overlapped zero (median $\beta = 0.04$, 95% CI = −0.32, 0.37; Table S2), indicating no detectable difference in the total GERP load of yearlings and adults (Figure 1C).

We then applied the same modeling approach to deleterious mutations predicted using SnpEff. In both models, the 95% CIs of the posterior β estimates of age overlapped zero (early-life model, median $\beta = -0.17$, 95% CI = −0.49, 0.15; Figure 1B; Table S2; late-life model, median $\beta = 0.15$, 95% CI = −0.20, 0.50; Figure 1C; Table S2), indicating no evidence of viability selection against deleterious SnpEff mutations at either life-history stage. This is consistent with our previous findings for male reproductive success and likely reflects conceptual and methodological differences between the two prediction approaches.[6] Specifically, differences in their underlying assumptions may explain the lack of congruence between the two prediction approaches and the disparity in the number of mutations classified as deleterious, as previously discussed by Chen et al.[6]

Finally, to determine whether viability selection acts predominantly against homozygous deleterious mutations, we modified the Bayesian LMMs described above by replacing the total load with the homozygous load, separately for deleterious mutations identified by GERP and SnpEff. In the early-life model, the 95% CI of the posterior β estimates of age marginally overlapped zero for the homozygous GERP load (median $\beta = 0.27$, 95% CI = −0.04, 0.59), hinting at a possible trend toward higher homozygous GERP loads in chicks compared with yearlings and adults. The 95% CIs of the posterior β estimates of age also overlapped zero in the late-life model for the homozygous GERP load (median $\beta = -0.22$, 95% CI = −0.56, 0.13) and in both models for the homozygous SnpEff load (early-life model: median $\beta = 0.12$, 95% CI = −0.22, 0.43; late-life model: median $\beta = 0.22$, 95% CI = −0.14, 0.57). Overall, these results are similar, though somewhat weaker, than those based on the total load, consistent with the theoretical expectation[4] and our previous finding[6] that both homozygous and heterozygous mutations contribute to the overall mutation load.

Early-life viability selection acts against deleterious mutations in exons

The genome is composed of functionally diverse elements, leading to heterogeneity in the strength and direction of selection across different genomic regions.[6] For example, coding (exonic) mutations can alter amino acid sequences and disrupt protein structure and function,[20,21] while non-coding (promoter and intronic) mutations can impair gene regulation and the ability to dynamically adjust gene expression to meet context-dependent functional demands.[7] We investigated whether viability selection differs across genomic regions by annotating deleterious GERP mutations according to their location within exons ($n = 28{,}100$), promoters ($n = 20{,}898$) or introns ($n = 113{,}578$) and calculating the total GERP load separately for each region. The resulting region-specific GERP loads were then fitted as response variables in Bayesian LMMs with the same model structure described above. This analysis was restricted to GERP mutations, as no evidence was found of viability selection acting against deleterious mutations predicted by SnpEff.

In the early-life models, the posterior β estimates of age were consistently positive for the total GERP load in exons, with a median β of 0.99 (95% CI = 0.69, 1.29; Table S2), indicating that chicks carry significantly more deleterious exonic mutations than older individuals (Figure 2). By contrast, the 95% CIs of the posterior β estimates of age overlapped zero for the total GERP load in promoters (median $\beta = 0.15$, 95% CI = −0.18, 0.47; Table S2; Figure 2) and introns (median $\beta = -0.01$, 95% CI = −0.30, 0.31; Table S2; Figure 2), indicating no detectable differences in these regions. In the late-life models, the 95% CIs of the posterior β estimates of age overlapped zero for total GERP load in exons, promoters, and introns (Table S2), indicating no evidence of viability selection in later life. Together, these results suggest that early-life viability selection predominantly targets deleterious mutations located in exons.

DISCUSSION

Predicted deleterious mutations theoretically reduce fitness, yet their realized effects in wild populations remain poorly understood.[4,22,23] Notably, studies of inbreeding depression typically overlook the fitness effects of heterozygous deleterious mutations, whereas the combined effects of selection across different life-history stages and genomic regions are seldom investigated. We therefore quantified viability selection against predicted deleterious mutations across life-history stages and genomic regions in a wild population of black grouse. We found that viability selection is strongest early in life and predominantly targets mutations at evolutionarily conserved sites in exons. This pattern is consistent with the expectation that early development is a period of heightened selection during which coding mutations that disrupt essential biological processes are preferentially filtered out of the population.

Theory predicts that viability selection should be strongest early in life,[24] as mutations disrupting essential genes involved in development or somatic maintenance are more likely to manifest during early ontogeny, reducing survival[25] and leading to weaker purifying selection later in life.[24,26] Conversely, mutations affecting reproductive performance may only manifest after sexual maturity, allowing sexual selection to act against them at later stages.[26,27] Consistent with these predictions, we detected inbreeding depression for early- but not late-life survival, although this effect was relatively weak. This is probably

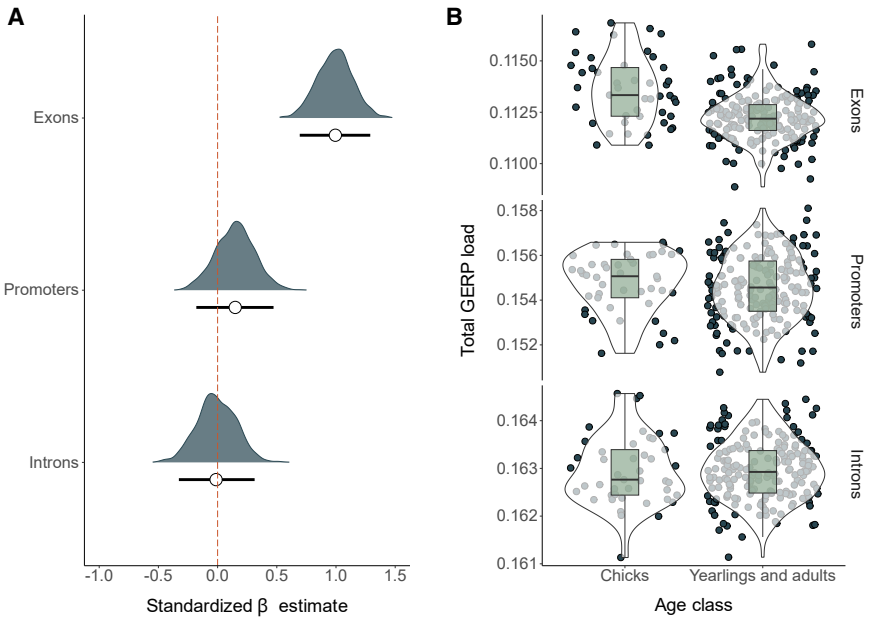

Figure 2. Differences in the total GERP load of chicks and older individuals, stratified by genomic region

(A) Posterior distributions of the standardized β estimates of age (chicks compared with yearlings and adults combined) on the total GERP load, calculated separately for exons, promoters, and introns (top to bottom). The white circles represent the median posterior estimates and the horizontal black lines the 95% CIs.

(B) Scatterplots of the total GERP load of chicks versus older individuals, calculated separately for exons, promoters, and introns (top to bottom). Violin plots indicate the density of the data. Thick horizontal lines indicate the median total GERP loads, whereas the lower and upper hinges correspond to the first and third quartiles, respectively, and the whiskers represent 1.5 times the interquartile range.

See also Table S2.

because inbreeding depression only captures the fitness effects of homozygous deleterious recessive mutations, while missing the substantial fitness costs associated with the expression of the heterozygous load. Supporting this interpretation, we found that deleterious mutations predicted using evolutionary conservation exhibited a stronger signal of viability selection than genomic inbreeding.

Understanding how deleterious mutations affect fitness is essential for elucidating how natural selection operates and for assessing extinction risks in small or declining populations. We found that early-life viability selection acts most strongly against predicted deleterious mutations located in exons. This suggests that disruptions to protein structure and function are particularly detrimental to early survival, presumably because they impair normal development, immune function, and/or somatic maintenance. Our findings support classic mutation load theory, which argues that mutations impairing protein function, especially those affecting functionally important genes, are likely to be harmful.[1,28] Moreover, the observed pattern of stronger selection in early life is consistent with indirect evidence from model organisms indicating that the efficacy of purifying selection declines with age, as reflected by changes in the ratio of synonymous to nonsynonymous mutations.[29]

Our finding that viability selection acts predominantly against deleterious mutations located in exonic regions contrasts sharply with our previous study of the same population showing that sexual selection acts mainly against deleterious mutations residing in regulatory regions.[6] This suggests that viability selection and sexual selection may act on largely distinct sets of mutations, with viability selection targeting mutations that disrupt protein synthesis and structure, and sexual selection acting against mutations that impair the regulation of gene expression in response to context-dependent demands. This difference may arise because traits related to survival depend on stable biological functions, whereas reproductive success in black grouse is strongly influenced by behavior,[6] a highly dynamic trait that requires fine-scale and time-sensitive gene regulation in response to internal and external stimuli.[30,31]

Overall, our study provides clear empirical evidence that selection against deleterious mutations can be temporally and functionally heterogenous in a wild population. Our results have important implications for evolutionary and life-history theory. First, they suggest that the fitness effects of mutations are not fixed but can vary depending on the trait measured and the specific biological context, such as life-history stage. Second, our findings indicate that the efficacy of purging deleterious mutations may differ among mutation types, with coding mutations appearing more strongly impacted by early-life viability selection than regulatory mutations.

Our findings also have implications for conservation genomics. Genomic mutation load estimates are increasingly used in endangered species to assess extinction risk[32] and inform conservation strategies.[23] However, this approach relies on the assumption that predicted deleterious mutations indeed reduce individual fitness and population viability, a link that has received only partial empirical validation and remains an active area of investigation.[6,33,34] Moreover, genomic mutation load estimates are typically calculated across the entire genome, without distinguishing between different types of mutations or accounting for life-history stage-specific effects. In our study, predicted deleterious mutations explained fitness variation, depending on the prediction approach used, and their effects differed between coding and non-coding mutations as well as across life-history stages. These findings highlight the importance of developing more nuanced approaches that integrate life-history data and consider when, where, and how deleterious mutations exert their effects. More broadly, our study demonstrates how bioinformatic tools can be used to investigate the evolutionary dynamics of wild populations and the proximate mechanisms underlying individual fitness variation.

RESOURCE AVAILABILITY

Lead contact

Further information and requests for resources and reagents should be directed to, and will be fulfilled by, the lead contact, Rebecca S. Chen (rebecca.chen@uni-bielefeld.de).

Materials availability

This study did not generate any new, unique reagents.

Data and code availability

- Whole-genome resequencing data can be found under NCBI BioProject PRJNA1085187 with SRA BioAccession numbers SRX29497999–SRX29498044 (chicks) and SRX24126841–SRX24127030 (yearlings and adults).
- All original code and intermediate files have been deposited on Zenodo.[35]
- Any additional information required to reanalyze the data reported in this paper is available from the lead contact upon request.

ACKNOWLEDGMENTS

We thank the many researchers that collected the field data used for this study, including Panu Halme, Matti Halonen, Tuomo Pihlaja, Elina Rantanen, Christophe Lebigre, and Matti Kervinen. We also gratefully acknowledge Professor Rauno V. Alatalo for initiating the black grouse project and Dr. Heli Siitari for sustaining the project after his retirement and passing. Lastly, we would like to thank Kateryna Firsova for producing the black grouse artwork used in Figure 1. This research was supported by a Deutsche Forschungsgemeinschaft (DFG) grant awarded to J.I.H. (HO 5122/14-1, project number 454606304), the Academy of Finland (grant nos. 7211271 and 7119165), and the Finnish Centre of Excellence in Evolutionary Research (Academy of Finland).

AUTHOR CONTRIBUTIONS

Conceptualization, R.S.C., C.D.S., and J.I.H.; methodology, R.S.C. and C.D.S.; investigation, R.S.C.; writing – original draft, R.S.C. and J.I.H.; writing – review & editing, all authors; funding acquisition, C.D.S., K.v.O., and J.I.H.; resources, C.D.S.; supervision, C.D.S., K.v.O., and J.I.H.

DECLARATION OF INTERESTS

The authors declare no competing interests.

STAR★METHODS

Detailed methods are provided in the online version of this paper and include the following:

- KEY RESOURCES TABLE
- EXPERIMENTAL MODEL AND STUDY PARTICIPANT DETAILS
- METHOD DETAILS
  - DNA extraction and genotyping
  - Genetic recapture analysis
  - Genomic Inbreeding
  - Variant prediction
  - Genomic mutation loads
- QUANTIFICATION AND STATISTICAL ANALYSIS

SUPPLEMENTAL INFORMATION

Supplemental information can be found online at https://doi.org/10.1016/j.cub.2025.10.043.

Received: July 29, 2025
Revised: September 5, 2025
Accepted: October 14, 2025
Published: November 18, 2025

REFERENCES

1. Muller, H.J. (1950). Our load of mutations. Am. J. Hum. Genet. *2*, 111–176.
2. Agrawal, A.F., and Whitlock, M.C. (2012). Mutation load: the fitness of individuals in populations where deleterious alleles are abundant. Annu. Rev. Ecol. Evol. Syst. *43*, 115–135. https://doi.org/10.1146/annurev-ecolsys-110411-160257.
3. Charlesworth, D., and Willis, J.H. (2009). The genetics of inbreeding depression. Nat. Rev. Genet. *10*, 783–796. https://doi.org/10.1038/nrg2664.
4. Bertorelle, G., Raffini, F., Bosse, M., Bortoluzzi, C., Iannucci, A., Trucchi, E., Morales, H.E., and van Oosterhout, C. (2022). Genetic load: genomic estimates and applications in non-model animals. Nat. Rev. Genet. *23*, 492–503. https://doi.org/10.1038/s41576-022-00448-x.
5. Morton, N.E., Crow, J.F., and Muller, H.J. (1956). An estimate of the mutational damage in man from data on consanguineous marriages. Proc. Natl. Acad. Sci. USA *42*, 855–863. https://doi.org/10.1073/pnas.42.11.855.
6. Chen, R.S., Soulsbury, C.D., Hench, K., Van Oers, K., and Hoffman, J.I. (2025). Predicted deleterious mutations reveal the genetic architecture of male reproductive success in a lekking bird. Nat. Ecol. Evol. *9*, 1924–1937. https://doi.org/10.1038/s41559-025-02802-8.
7. Wray, G.A. (2007). The evolutionary significance of cis-regulatory mutations. Nat. Rev. Genet. *8*, 206–216. https://doi.org/10.1038/nrg2063.
8. Hemmings, N.L., Slate, J., and Birkhead, T.R. (2012). Inbreeding causes early death in a passerine bird. Nat. Commun. *3*, 863. https://doi.org/10.1038/ncomms1870.
9. Stoffel, M.A., Johnston, S.E., Pilkington, J.G., and Pemberton, J.M. (2021). Genetic architecture and lifetime dynamics of inbreeding depression in a wild mammal. Nat. Commun. *12*, 2972. https://doi.org/10.1038/s41467-021-23222-9.
10. Davydov, E.V., Goode, D.L., Sirota, M., Cooper, G.M., Sidow, A., and Batzoglou, S. (2010). Identifying a high fraction of the human genome to be under selective constraint using GERP++. PLOS Comput. Biol. *6*, e1001025. https://doi.org/10.1371/journal.pcbi.1001025.
11. Cingolani, P., Platts, A., Wang, L.L., Coon, M., Nguyen, T., Wang, L., Land, S.J., Lu, X., and Ruden, D.M. (2012). A program for annotating and predicting the effects of single nucleotide polymorphisms, SnpEff: SNPs in the genome of Drosophila melanogaster strain w1118; iso-2; iso-3. Fly *6*, 80–92. https://doi.org/10.4161/fly.19695.
12. Lindén, H. (1983). Metson ja teeren kuolevuudesta. Suomen Riista *30*, 79–89.
13. Caizergues, A., and Ellison, L.N. (2002). Natal dispersal and its consequences in Black Grouse Tetrao tetrix: Natal dispersal and its consequences in Black Grouse. Ibis *144*, 478–487. https://doi.org/10.1046/j.1474-919X.2002.00040.x.
14. Corrales, C., and Höglund, J. (2012). Maintenance of gene flow by female-biased dispersal of Black Grouse Tetrao tetrix in northern Sweden. J. Ornithol. *153*, 1127–1139. https://doi.org/10.1007/s10336-012-0844-0.
15. Lebigre, C., Alatalo, R.V., and Siitari, H. (2010). Female-biased dispersal alone can reduce the occurrence of inbreeding in black grouse (*Tetrao tetrix*). Mol. Ecol. *19*, 1929–1939. https://doi.org/10.1111/j.1365-294X.2010.04614.x.
16. Kervinen, M., Alatalo, R.V., Lebigre, C., Siitari, H., and Soulsbury, C.D. (2012). Determinants of yearling male lekking effort and mating success in black grouse (*Tetrao tetrix*). Behav. Ecol. *23*, 1209–1217. https://doi.org/10.1093/beheco/ars104.
17. Caizergues, A., and Ellison, L.N. (1997). Survival of black grouse *Tetrao tetrix* in the French Alps. Wildl. Biol. *3*, 177–186. https://doi.org/10.2981/wlb.1997.022.
18. Warren, P.K., and Baines, D. (2002). Dispersal, survival and causes of mortality in black grouse Tetrao tetrix in northern England. Wildl. Biol. *8*, 91–97. https://doi.org/10.2981/wlb.2002.013.

19. Pekkola, M., Alatalo, R., Pöysä, H., and Siitari, H. (2014). Seasonal survival of young and adult black grouse females in boreal forests. Eur. J. Wildl. Res. *60*, 477–488. https://doi.org/10.1007/s10344-014-0809-0.

20. Zhang, Z., Miteva, M.A., Wang, L., and Alexov, E. (2012). Analyzing effects of naturally occurring missense mutations. Comp. Math. Methods Med. *2012*, 805827. https://doi.org/10.1155/2012/805827.

21. DePristo, M.A., Weinreich, D.M., and Hartl, D.L. (2005). Missense meanderings in sequence space: a biophysical view of protein evolution. Nat. Rev. Genet. *6*, 678–687. https://doi.org/10.1038/nrg1672.

22. Dussex, N., van der Valk, T., Morales, H.E., Wheat, C.W., Díez-del-Molino, D., von Seth, J., Foster, Y., Kutschera, V.E., Guschanski, K., Rhie, A., et al. (2021). Population genomics of the critically endangered kākāpō. Cell Genomics *1*, 100002. https://doi.org/10.1016/j.xgen.2021.100002.

23. Kardos, M., Keller, L.F., and Funk, W.C. (2024). What can genome sequence data reveal about population viability? Mol. Ecol. e17608. https://doi.org/10.1111/mec.17608.

24. Medawar, P.B. (1952). An Unsolved Problem of Biology (H.K. Lewis & Co.).

25. Keller, L., and Waller, M. (2002). Inbreeding effects in wild populations. Trends Ecol. Evol. *17*, 230–241. https://doi.org/10.1016/S0169-5347(02)02489-8.

26. Hamilton, W.D. (1966). The moulding of senescence by natural selection. J. Theor. Biol. *12*, 12–45. https://doi.org/10.1016/0022-5193(66)90184-6.

27. Williams, G.C. (1957). Pleiotropy, natural selection, and the evolution of senescence. Evolution *11*, 398–411. https://doi.org/10.1111/j.1558-5646.1957.tb02911.x.

28. Kimura, M. (1968). Evolutionary rate at the molecular level. Nature *217*, 624–626. https://doi.org/10.1038/217624a0.

29. Cheng, C., and Kirkpatrick, M. (2021). Molecular evolution and the decline of purifying selection with age. Nat. Commun. *12*, 2657. https://doi.org/10.1038/s41467-021-22981-9.

30. Bell, A.M., and Robinson, G.E. (2011). Genomics. Behavior and the dynamic genome. Science *332*, 1161–1162. https://doi.org/10.1126/science.1203295.

31. Rittschof, C.C., and Hughes, K.A. (2018). Advancing behavioural genomics by considering timescale. Nat. Commun. *9*, 489. https://doi.org/10.1038/s41467-018-02971-0.

32. Van Oosterhout, C. (2020). Mutation load is the spectre of species conservation. Nat. Ecol. Evol. *4*, 1004–1006. https://doi.org/10.1038/s41559-020-1204-8.

33. Hoffman, J.I., Vendrami, D.L.J., Hench, K., Chen, R.S., Stoffel, M.A., Kardos, M., Amos, W., Kalinowski, J., Rickert, D., Köhrer, K., et al. (2024). Genomic and fitness consequences of a near-extinction event in the northern elephant seal. Nat. Ecol. Evol. *8*, 2309–2324. https://doi.org/10.1038/s41559-024-02533-2.

34. Hasselgren, M., Dussex, N., Von Seth, J., Angerbjörn, A., Dalén, L., and Norén, K. (2024). Strongly deleterious mutations influence reproductive output and longevity in an endangered population. Nat. Commun. *15*, 8378. https://doi.org/10.1038/s41467-024-52741-4.

35. Chen, R. (2025). rshuhuachen/ms_chicks_viability. Zenodo. https://doi.org/10.5281/zenodo.17060609.

36. Andrews, S., Krueger, F., Segonds-Pichon, A., Biggins, L., Krueger, C., and Wingett, S. (2010). FastQC. Babraham Bioinformatics *370*. https://doi.org/10.4236/cs.2014.53007.

37. Li, H. (2013). Aligning sequence reads, clone sequences and assembly contigs with BWA-MEM. Preprint at arXiv. https://doi.org/10.48550/arXiv.1303.3997.

38. Danecek, P., Bonfield, J.K., Liddle, J., Marshall, J., Ohan, V., Pollard, M.O., Whitwham, A., Keane, T., McCarthy, S.A., Davies, R.M., et al. (2021). Twelve years of SAMtools and BCFtools. GigaScience *10*, giab008. https://doi.org/10.1093/gigascience/giab008.

39. Danecek, P., Auton, A., Abecasis, G., Albers, C.A., Banks, E., DePristo, M.A., Handsaker, R.E., Lunter, G., Marth, G.T., Sherry, S.T., et al. (2011). The variant call format and VCFtools. Bioinformatics *27*, 2156–2158. https://doi.org/10.1093/bioinformatics/btr330.

40. Purcell, S., Neale, B., Todd-Brown, K., Thomas, L., Ferreira, M.A.R., Bender, D., Maller, J., Sklar, P., de Bakker, P.I.W., Daly, M.J., et al. (2007). PLINK: a tool set for whole-genome association and population-based linkage analyses. Am. J. Hum. Genet. *81*, 559–575. https://doi.org/10.1086/519795.

41. Manichaikul, A., Mychaleckyj, J.C., Rich, S.S., Daly, K., Sale, M., and Chen, W.-M. (2010). Robust relationship inference in genome-wide association studies. Bioinformatics *26*, 2867–2873. https://doi.org/10.1093/bioinformatics/btq559.

42. Chen, R. (2025). rshuhuachen/ms_load_grouse: Release for NEE Publication. Zenodo. https://doi.org/10.5281/ZENODO.15608151.

43. Helminen, M. (1963). Composition of the Finnish populations of capercaillie, *Tetrao urogallus*, and black grouse, *Lyrurus tetrix*, in the autumns of 1952–1961, as revealed by a study of wings. Riistatiet Julk. *8*, 142–149.

44. Kervinen, M., Lebigre, C., and Soulsbury, C.D. (2016). Data from: Simultaneous Age-Dependent and Age-Independent Sexual Selection in the Lekking Black Grouse (Lyrurus tetrix). Dryad. https://doi.org/10.5061/DRYAD.2JJ6Q.

45. Ludwig, G.X., Alatalo, R.V., Helle, P., and Siitari, H. (2010). Individual and environmental determinants of daily Black Grouse nest survival rates at variable predator densities. Ann. Zool. Fenn. *47*, 387–397. https://doi.org/10.5735/086.047.0602.

46. Ludwig, G.X., Alatalo, R.V., Helle, P., Lindén, H., Lindström, J., and Siitari, H. (2006). Short- and long-term population dynamical consequences of asymmetric climate change in black grouse. Proc. Biol. Sci. *273*, 2009–2016. https://doi.org/10.1098/rspb.2006.3538.

47. Hannon, S.J., and Martin, K. (2006). Ecology of juvenile grouse during the transition to adulthood. J. Zool. *269*, 422–433. https://doi.org/10.1111/j.1469-7998.2006.00159.x.

48. Chen, S. (2023). Ultrafast one-pass FASTQ data preprocessing, quality control, and deduplication using fastp. Imeta *2*, e107. https://doi.org/10.1002/imt2.107.

49. Chen, Y., Chen, Y., Shi, C., Huang, Z., Zhang, Y., Li, S., Li, Y., Ye, J., Yu, C., Li, Z., et al. (2018). SOAPnuke: a MapReduce acceleration-supported software for integrated quality control and preprocessing of high-throughput sequencing data. GigaScience *7*, 1–6. https://doi.org/10.1093/gigascience/gix120.

50. Narasimhan, V., Danecek, P., Scally, A., Xue, Y., Tyler-Smith, C., and Durbin, R. (2016). BCFtools/RoH: a hidden Markov model approach for detecting autozygosity from next-generation sequencing data. Bioinformatics *32*, 1749–1751. https://doi.org/10.1093/bioinformatics/btw044.

51. Meyermans, R., Gorssen, W., Buys, N., and Janssens, S. (2020). How to study runs of homozygosity using PLINK? A guide for analyzing medium density SNP data in livestock and pet species. BMC Genomics *21*, 94. https://doi.org/10.1186/s12864-020-6463-x.

52. Armstrong, J., Hickey, G., Diekhans, M., Fiddes, I.T., Novak, A.M., Deran, A., Fang, Q., Xie, D., Feng, S., Stiller, J., et al. (2020). Progressive Cactus is a multiple-genome aligner for the thousand-genome era. Nature *587*, 246–251. https://doi.org/10.1038/s41586-020-2871-y.

53. Lawrence, M., Huber, W., Pagès, H., Aboyoun, P., Carlson, M., Gentleman, R., Morgan, M.T., and Carey, V.J. (2013). Software for computing and annotating genomic ranges. PLOS Comput. Biol. *9*, e1003118. https://doi.org/10.1371/journal.pcbi.1003118.

54. Lawrence, M., Gentleman, R., and Carey, V. (2009). rtracklayer: an R package for interfacing with genome browsers. Bioinformatics *25*, 1841–1842. https://doi.org/10.1093/bioinformatics/btp328.

55. Lindner, M., Laine, V.N., Verhagen, I., Viitaniemi, H.M., Visser, M.E., van Oers, K., and Husby, A. (2021). Rapid changes in DNA methylation associated with the initiation of reproduction in a small songbird. Mol. Ecol. *30*, 3645–3659. https://doi.org/10.1111/mec.15803.

56. Gabry, J., Simpson, D., Vehtari, A., Betancourt, M., and Gelman, A. (2019). Visualization in Bayesian workflow. J. R. Stat. Soc. A *182*, 389–402. https://doi.org/10.1111/rssa.12378.

57. Hespanhol, L., Vallio, C.S., Costa, L.M., and Saragiotto, B.T. (2019). Understanding and interpreting confidence and credible intervals around effect estimates. Braz. J. Phys. Ther. *23*, 290–301. https://doi.org/10.1016/j.bjpt.2018.12.006.

58. Team, R.C. (2021) R: A Language and Environment for Statistical Computing.

59. Posit team. (2024). R.Studio: Integrated Development Environment for R Posit Software (PBC).

60. Wickham, H., Averick, M., Bryan, J., Chang, W., McGowan, L., François, R., Grolemund, G., Hayes, A., Henry, L., Hester, J., et al. (2019). Welcome to the Tidyverse. JOSS *4*, 1686. https://doi.org/10.21105/joss.01686.

61. Wilke, C., Fox, S.J., Bates, T., Manalo, K., Lang, B., Barrett, M., Stoiber, M., Philipp, A., Denney, B., Hesselberth, J., et al. (2021). wilkelab/cowplot: 1.1.1. Zenodo. https://doi.org/10.5281/ZENODO.2533860.

62. Wilke, C.O. (2022). ggridges: Ridgeline Plots in "ggplot2." Version R package version 0.5.4. https://wilkelab.org/ggridges/.

63. Mölder, F., Jablonski, K.P., Letcher, B., Hall, M.B., van Dyken, P.C., Tomkins-Tinch, C.H., Sochat, V., Forster, J., Vieira, F.G., Meesters, C., et al. (2021). Sustainable data analysis with Snakemake. F1000Res *10*, 33. https://doi.org/10.12688/f1000research.29032.3.

64. Anaconda Software Distribution (2016), Version Vers. 2-2.4.0. https://anaconda.org/anaconda/anaconda-navigator/files?version=2.4.0&page=0.

65. Moreau, D., Wiebels, K., and Boettiger, C. (2023). Containers for computational reproducibility. Nat. Rev. Methods Primers *3*, 50. https://doi.org/10.1038/s43586-023-00236-9.

STAR★METHODS

KEY RESOURCES TABLE

REAGENT or RESOURCE	SOURCE	IDENTIFIER
Critical commercial assays		
DNeasy Blood & Tissue Kit	QIAGEN, Hilden, Germany	Cat #69504
MGIEasy Universal Library Conversion Kit (App-A) version 1.0	MGI	1000004155 (16 RXN)
VAHTSTM Universal Plus DNA Library Prep Kit for Illumina	VAHTSTM	ND617-02
VAHTSTM DNA Clean Beads	VAHTSTM	N411-03
Qubit TM dsDNA HS Assay Kit	Invitrogen	N/A
Deposited data		
Raw fastq reads chicks	This study	NCBI BioProject PRJNA1085187
Raw fastq reads yearlings and adults	Chen et al.[6]	NCBI BioProject PRJNA1085187
Oligonucleotides		
Adapter 3: "AGATCGGAAGAGCAC ACGTCTGAACTCCAGTCAC"	TruSeq Universal Adapter sequence	Illumina
Adapter 5: "AGATCGGAAGAGCGTC GTGTAGGGAAAGAGTGT"	TruSeq Universal Adapter sequence	Illumina
Software and algorithms		
SOAPnuke	Chen et al.[36]	https://github.com/BGI-flexlab/SOAPnuke
FastQC	Andrews et al.[37]	https://www.bioinformatics.babraham.ac.uk/projects/fastqc/
BWA	Li[38]	https://github.com/lh3/bwa
samtools	Danecek et al.[39]	https://www.htslib.org/
BCFtools	Danecek et al.[39]	https://github.com/samtools/bcftools
VCFtools	Danecek et al.[40]	https://vcftools.github.io/index.html
PLINK	Purcell et al.[41]	https://www.cog-genomics.org/plink/
GERP++	Davydov et al.[10]	https://pmc.ncbi.nlm.nih.gov/articles/PMC7286533/
SnpEff	Cingolani et al.[11]	https://pcingola.github.io/SnpEff/
Progressive Cactus	Armstrong et al.[42]	https://github.com/ComparativeGenomicsToolkit/cactus
brms	Bürkner[22]	https://paulbuerkner.com/brms/
Other		
Proteinase K	N/A	N/A

EXPERIMENTAL MODEL AND STUDY PARTICIPANT DETAILS

Five black grouse leks in Central Finland were monitored from 1999 to 2013 inclusive. Yearling and adult birds of both sexes were trapped prior to the lekking season, between January and March, using baited walk-in traps. 1–2 ml of blood was taken from yearlings and adults with a heparinized syringe from the brachial vein and stored at 4°C in 70% ethanol until DNA extraction. Individuals were aged as yearlings or adults based on their plumage characteristics.[43] Each bird was tagged with an aluminum tarsus ring carrying a unique serial number and three colored rings to allow for visual identification in the field. Yearlings and adult males were assumed to have died when they were never caught or sighted subsequently. We also collected life-history data and blood samples from 190 adult male black grouse as part of earlier studies.[6,44] All fieldwork was ethically approved by the Central Finland Environmental Centre (permissions KSU-2003-L-25/254 and KSU-2002-L4/254) with additional permissions for specific sites (KSU-2004-L-72/254).

During capture prior to the lekking season, adult females were fitted with necklace-mounted radio transmitters to enable their nests to be located at the start of incubation via radiotracking as described by Ludwig et al.[45] Nests were visited on or near the estimated hatching date, which was inferred by floating the eggs in lukewarm water.[45] On the estimated day of hatching, the chicks were

located either in the nest or nearby and were captured just after hatching, before they moved away from the nest. Blood samples (2 x 70 μl capillary tubes per individual) were taken from the brachial vein of the chicks. Because the chick's tarsi were too small and grow too rapidly to allow safe ringing at this stage, individual identification over time was not possible. Consequently, some chicks could have been inadvertedly resampled at later life-history stages. However, given the low survival rate of chicks (11%-17%[12]), with the highest mortality occurring within the first two weeks post-hatching,[46,47] and because males generally do not disperse,[13–15] the majority of chicks were assumed to have died. Thus, our estimate of early-life viability selection may be conservative; if any sampled chicks survived to the yearling stage, the strength of viability selection would likely be underestimated.

METHOD DETAILS

DNA extraction and genotyping

DNA was extracted from red blood cells using either a Qiagen Blood and Tissue Extraction Kit (n = 208) or a standard chloroform-isoamyl alcohol protocol (n = 28). To minimize familial effects, one male chick was randomly selected from each brood (n = 46) for analysis. A single library was prepared for all 46 selected chick samples by Biomarker Technologies (BMK) GmbH using the VAHTS Universal Plus DNA Library Prep Kit for Illumina (ND617) following the manufacturer's protocol. Fragmented and end repaired DNA was size-selected using magnetic beads, followed by adapter ligation and clean-up using VAHTS DNA Clean Beads. The library was amplified using polymerase chain reaction (PCR) and subjected to quality control. Fragment sizes were assessed using a Qsep-400 and DNA concentrations were quantified using a Qubit 3.0. Whole genome (150bp paired-end) sequencing of all the chick samples was conducted on a single Illumina NovaSeq X Plus lane at the Beijing Genomics Institute (BGI). Adaptor sequences and low-quality reads (those with average quality scores below 20) were removed using fastp v1.0.[48]

Library preparation of the yearling and adult samples was performed at the Beijing Genomics Institute using the BGI Optimal DNA Library Prep Kit as described elsewhere.[6] In brief, fragmented DNA was size-selected using magnetic beads and end-repaired, followed by adapter ligation and PCR amplification. The resulting double stranded DNA was denatured and a circularization reaction was used to generate single-stranded circularized libraries. The whole genomes of all (sub)adults were 150bp paired-end sequenced in eight DNBSEQ-G400 lanes. The adaptor sequences were removed and low quality reads and contamination were excluded using SOAPnuke.[49]

The quality of the raw sequence reads was checked using FastQC v0.11.9.[36] Pre-processed reads were aligned to the scaffolded black grouse reference genome (NCBI RefSeq assembly GCA_043882375.1) using the Burrows-Wheeler alignment (BWA-*mem*) algorithm v0.7.13.[37] The resulting SAM files were converted to binary format (BAM) and subsequently sorted and indexed using samtools v1.15.1.[38] Single nucleotide polymorphisms (SNPs) were genotyped using the BCFtools *mpileup* command v1.11[38] and filtered for genotypes with a minimum quality of 20 (-q 20). Reads with excessive mismatches were penalised (-C 50). Additional filtering steps were implemented using vcftools v0.1.17.[39] We retained only biallelic SNPs (–min-alleles 2, –max-alleles 2), excluded indels (–remove-indels), and filtered for a minimum depth of coverage of 20x (–minDP 20) and a maximum depth of 58x (twice the mean depth, –max-meanDP 58). Variants with more than 30% missing data (–max-missing 0.7), or a quality score below 30 (–minQC 30) were excluded.

Genetic recapture analysis

Because the chicks were too young to be ringed at the time of sampling, we were unable to track their survival to the yearling stage as described above. Consequently, one or more chicks may have been inadvertedly resampled as yearlings or adults, potentially resulting in duplicate genotypes in our dataset. To identify such cases, we quantified pairwise relatedness among samples and considered any pair to represent the same individual if their relatedness exceeded the theoretical expectation for first degree relatives. We first filtered the dataset using PLINK v1.90[40] to remove: (i) strongly linked SNPs, where linkage disequilibrium (LD) was computed in window sizes of 50 bp with a step size of five SNPs and a variance inflation factor threshold of two (–indep 50 5 2); (ii) SNPs deviating significantly from Hardy-Weinberg equilibrium with an alpha level of 0.001 (–hwe 0.001); and (iii) SNPs with a minor allele frequency below 0.01 (–maf 0.01). We then calculated the relatedness coefficients $\hat{p}$, Z0, Z1 and Z2 using the -genome function in PLINK.[40] $\hat{p}$ is the overall proportion of the genome that is identical by descent (IBD) between any pair of individuals. Z0, Z1 and Z2 are coefficients that estimate the proportion of the genome for which zero, one or two alleles of a pair of individuals are IBD, respectively. Relatedness coefficients were assigned to each pair of individuals based on the thresholds described by Manichaikul et al.[41] Using this approach, we identified a single pair of individuals (chick C06 and adult D229192) whose relatedness ($\hat{p}$ = 0.96) exceeded the theoretical expectations for both parent-offspring and full-sibling relationships ($\hat{p}$ = 0.50). As a conservative measure, we therefore excluded chick C06 from further analyses, as our results suggest that it may have survived to the yearling stage.

Genomic Inbreeding

Runs of homozygosity (ROHs) were called using BCFtools v1.11.[50] The BCFtools algorithm uses a hidden Markov model to detect regions of autozygosity by assessing the likelihood that two alleles are identical by descent. This algorithm therefore does not rely on settings of parameters needed for ROH detection software like PLINK[51] that use sliding windows.[50] We only used genotypes with a minimum quality of 30 (–G30) to call ROHs with the default allele frequency settings. The raw output from BCFtools was filtered to

include only ROHs with a quality score over 30, a minimum length of at least 100kb, and containing at least 100 SNPs. Next, we calculated F_{ROH} as the proportion of the autosomal genome in ROHs). The sex scaffold was identified as described by Chen et al.[6] and excluded from the calculation of F_{ROH}.

Variant prediction

To identify putatively deleterious mutations, we first inferred the ancestral state of each site in the genome using the reconstructed genome of the last common ancestor of the black grouse and the white-tailed ptarmigan, and derived alleles were assumed to be deleterious (see Chen et al.[6] for additional details). Putatively deleterious mutations were then identified using GERP[10] and SnpEff.[11]

GERP++ was used to estimate evolutionary constraint from a multi-species alignment by calculating GERP scores across the genome, which reflect the deficit of substitutions at a given site compared to neutral expectations. High GERP scores indicate stronger evolutionary constraint, implying that mutations at these sites are more likely to be more deleterious. We constructed a multi-species alignment of 74 avian genomes using Progressive Cactus v2.6.12[52] and calculated GERP scores using GERP++[10] as described by Chen et al.[6] GERP scores were computed for the 29 largest autosomal scaffolds using the default settings, with the -d flag enabled to exclude the focal reference genome and reduce bias. Following Chen et al.,[6] we defined a deleterious GERP mutation as a derived allele at a locus with a GERP score ≥ 4.

SnpEff predicts the effect of a mutation on protein structure and function.[11] Each variant is classified into one of four impact categories: high, moderate, low and modifier. High impact mutations are predicted to have the most severe functional effects and include LOF mutations. To annotate genetic variants in our population, we used SnpEff in combination with the black grouse genome annotation (available via GitHub[42]) as described by Chen et al.[6] We built a custom black grouse database, annotated each mutation, and then used SnpSift[11] to extract mutations located in the 29 largest autosomal scaffolds annotated as high impact. We defined a deleterious SnpEff mutation as a derived allele at a locus annotated as having a high impact.

Genomic mutation loads

Each individual's total genomic mutation load was quantified as the number of deleterious alleles (counting two for homozygous derived mutations and one for heterozygous derived mutations) divided by the number of successfully genotyped loci carrying a deleterious allele, as described by Chen et al.[6] This calculation was performed separately for loci identified as deleterious based on GERP and SnpEff predictions, resulting in two independent genomic mutation load estimates, herein referred to as the "total GERP load" and the "total SnpEff load" respectively.

To test for spatial variation in the mutation load, we constructed Bayesian linear models using the R package stats brms v2.19.0,[7] with either the total GERP load or the total SnpEff load fitted as the response variable and lekking site fitted as a 5-level fixed effect predictor variable (Figure S2; Table S1). To test for temporal variation, we constructed analogous models with birth year fitted as a 10-level fixed effect predictor variable (Figure S2; Table S1). This analysis was based on chicks, yearlings and adults combined.

QUANTIFICATION AND STATISTICAL ANALYSIS

First, we quantified inbreeding depression for survival using Bayesian linear mixed effect models (LMMs) constructed with the R package brms v2.19.0.[7] We tested for inbreeding depression in early-life by constructing a model of F_{ROH} with age (chicks versus yearlings plus adults combined, $n = 235$ animals) fitted as a two-level fixed effect predictor variable. We tested for inbreeding depression in late-life by constructing a model of F_{ROH} with age (yearlings versus adults, $n = 190$ animals) fitted as a two-level fixed effect predictor variable. F_{ROH} estimates were z-transformed and lekking site was included as a random effect in the models to account for potential site-specific demographic variation.

Next, to quantify viability selection against predicted deleterious mutations, we modified the Bayesian LMMs described above by replacing F_{ROH} with the z-transformed total GERP load or the z-transformed total SnpEff load as the response variables respectively. Separate models were again constructed for early- and late-life viability selection for each mutation load type, with lekking site included as a random effect.

Finally, we evaluated whether viability selection acts more strongly on specific genomic regions. Each mutation was annotated to determine whether it overlapped a promoter, intron or exon using the R packages GenomicFeatures v1.42.3[53] and rtracklayer v1.50.0.[54] Promotors were defined as regions spanning from 2,000 bp upstream to 200 bp downstream of the gene's annotated transcription start site.[55] We then calculated the total mutation load separately for each genomic region and constructed six Bayesian LMMs as described above, one for each genomic region, stratified by life-history stage comparison. As before, the mutation load estimates were z-transformed and the models included the same fixed and random effects described above. This analysis was restricted to deleterious mutations identified by GERP, as we found no evidence of viability selection acting against high impact mutations predicted by SnpEff.

All of the Bayesian models were run for one million iterations across four independent Markov chains, with a warm-up phase of 500,000 iterations and a thinning interval of 1,000. Generic weakly informative priors were used for the population-level effects (normal distribution, mean = 0, SD = 1). To assess sensitivity to the choice of priors, we repeated all of the models using both the default brms priors and with an alternative prior specification (population-level effects: mean = 10, SD = 10; intercept: mean = 30, SD = 10). The results were comparable, indicating that our results and conclusions are robust to the choice of priors. Model performance was evaluated by checking for divergent transitions and convergence, as well as through the visual inspection

of autocorrelation plots, R hat statistics and effective sample sizes using the R package bayesplot v1.10.0.[56] Results were considered statistically significant if the 95% CI of the β estimate did not overlap zero.[57] Statistical parameters are reported in Tables S1 and S2.

All statistical analyses were implemented in R v4.5.1[58] using Rstudio v2025.05.0[59] and the results were visualized using the R packages ggplot2 v3.5.2,[60] cowplot v1.2.0,[61] bayesplot v1.13.0,[56] and ggridges v0.5.6.[62] The majority of bioinformatic workflows were integrated into Snakemake v7.14[63] using a conda environment[64] for enhanced reproducibility.[65]